

# Reducing Thermal Carrier Spreading in InP Quantum Dot Lasers

Makarimi Kasim, Stella N. Elliott, Andrey B. Krysa, and Peter M. Smowton, *Senior Member, IEEE*

**Abstract**—Record low values in this material system of threshold current density, particularly at elevated temperature, are presented for InP quantum dot lasers. Lasers with  $\text{Ga}_{0.58}\text{In}_{0.42}\text{P}$  in the dot upper confining layer have the lowest threshold current densities,  $138 \text{ A}\cdot\text{cm}^{-2}$  at 300 K, and  $235 \text{ A}\cdot\text{cm}^{-2}$  at 350 K (77 °C) (2-mm lasers, uncoated facets). Gain-current density data suggests laser performance with an upper confining layer of  $\text{Ga}_x\text{In}_{1-x}\text{P}$  with  $x = 0.54, 0.56$  or  $0.58$  would be similar if not for the very low internal optical mode loss,  $\alpha_i$ , of samples with  $x = 0.56$  and  $0.58$ . Gain measurements at fixed inversion level suggest that increasing  $x$  content in  $\text{Ga}_x\text{In}_{1-x}\text{P}$  increases gain at fixed inversion level but samples with  $x = 0.54$  also exhibit reduced recombination current density. The increasing recombination current density at elevated temperature due to thermal carrier spreading is significantly reduced in samples with  $x = 0.56$  and  $x = 0.58$  but measurements at common operating points attribute this largely to the reduced  $\alpha_i$  for these samples and given the same  $\alpha_i$ , samples with  $x = 0.54, 0.56$  and  $0.58$  would all benefit from reduced effects due to thermal carrier spreading compared to  $x = 0.52$ .

**Index Terms**—Quantum dot devices, semiconductor laser, short wavelength lasers, threshold current density, temperature sensitivity, InP self-assembled quantum dots.

## I. INTRODUCTION

INP quantum dots (QDs) grown on GaAs substrates are of interest because they can address wavelengths in the 630–750 nm range [1]–[3] and are important, for example, in biophotonic applications, where operation in the red/near I.R. allows good tissue penetration and minimisation of auto-fluorescence. However, to make these devices practical further improvements are required in threshold current at elevated temperature.

In previous work it has been shown that the reduction in gain caused by thermal carrier spreading over the inhomogeneously broadened QD states has a significant effect on the temperature dependence of threshold current density in InP QD lasers, [4] and that such effects are not significant in quantum well (QW) lasers operating in a similar part of the wavelength spectrum and fabricated from similar materials. These effects are also important in InAs QD lasers operating at telecom and datacom wavelengths although the absolute values of thresholds in the mature InAs QD system are much lower than those in the

InP/QD lasers. The concepts underlying these effects are readily understood. At elevated temperatures the population of states producing gain are governed by overall system charge neutrality and Fermi–Dirac statistics. In self assembled QD systems where small numbers of dot states are in close proximity to large numbers of QW and bulk states this can lead to severe gain saturation [5]. This effect is exacerbated by increase in the energy range of the carriers either with temperature or with increased pumping requirement if internal loss is not kept very low. Modifying the composition and thickness of the layer above the QDs produces changes in strain and state distribution [6]–[8] and can reduce the asymmetry in the QW states close to the dot states. In InP dot structures increasing the gallium content in the layer above the dots—the upper confining layer (UCL)—has resulted in improved threshold current and temperature dependence of threshold current density [9].

In this paper we demonstrate further reductions in high temperature threshold current density using strain in the UCL and perform a detailed experimental study to determine the major factors contributing to the performance achieved, one of which will prove to be the low value of scattering loss. In doing this we aim to reveal the intrinsic performance allowing optimization of future designs. We note that all self-assembled dot lasers, such as the InAs QDs, which are suitable for use in telecom and datacom applications, are governed by similar physics.

After describing the structures and threshold current data in part II we begin with measurements reflecting the state distribution and basic gain performance in part III before describing measurements to differentiate the factors that affect the temperature dependence of threshold current in part IV. We conclude in part V.

## II. DEVICE STRUCTURES

The structures were grown by low pressure metal organic vapor phase epitaxy on n-GaAs (1 0 0) substrate oriented  $10^\circ$  off toward  $\langle 1 1 1 \rangle$  using trimethyl precursors for the group III elements and arsine  $\text{AsH}_3$  and phosphine  $\text{PH}_3$  as precursors of the group V elements. Five layer active regions were created from self-assembled dots in a structure similar to dots-in-a-well [10] (DWELL). Each DWELL consisted of dots formed from the equivalent of 2.5 monolayers of InP material deposited on 16 nm of  $(\text{Al}_{0.3}\text{Ga}_{0.7})_{0.51}\text{In}_{0.49}\text{P}$  and covered with 8 nm  $\text{Ga}_x\text{In}_{1-x}\text{P}$  QW, where values of  $x$  of 0.52, 0.54, 0.56 and 0.58 were employed. The active regions were grown at a temperature of 730 °C. 1000 nm wide  $\text{Al}_{0.51}\text{In}_{0.49}\text{P}$  cladding layers, doped with Si and Zn for n- and p-type respectively, form the rest of the waveguide structure. The structure is represented schematically in Fig. 1.

The samples are fabricated into 50  $\mu\text{m}$  wide oxide isolated stripe lasers and segmented contact test structures. All devices

Manuscript received November 18, 2014; revised January 30, 2015; accepted February 9, 2015. This work was supported by the U.K. Engineering and Physical Sciences Research Council under Grant EP/L005409/1.

M. Kasim, S. N. Elliott, and P. M. Smowton are with the School of Physics and Astronomy, Cardiff University, Cardiff CF24 3AA, U.K. (e-mail: HjAwgKasimA@Cardiff.ac.uk; ElliottS1@Cardiff.ac.uk; SmowtonPM@cardiff.ac.uk).

A. B. Krysa is with the EPSRC National Centre for III-V Technologies, University of Sheffield, Sheffield S1 3JD, U.K. (e-mail: a.krysa@sheffield.ac.uk).

Color versions of one or more of the figures in this paper are available online at <http://ieeexplore.ieee.org>.

Digital Object Identifier 10.1109/JSTQE.2015.2403716

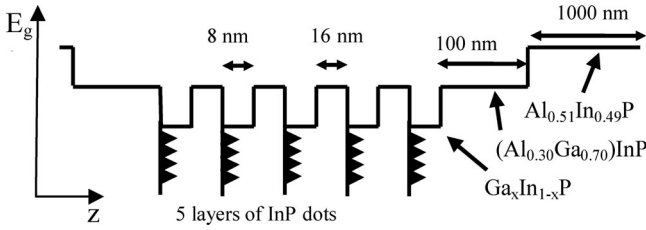


Fig. 1. Schema of energy gap along growth direction (not to scale).

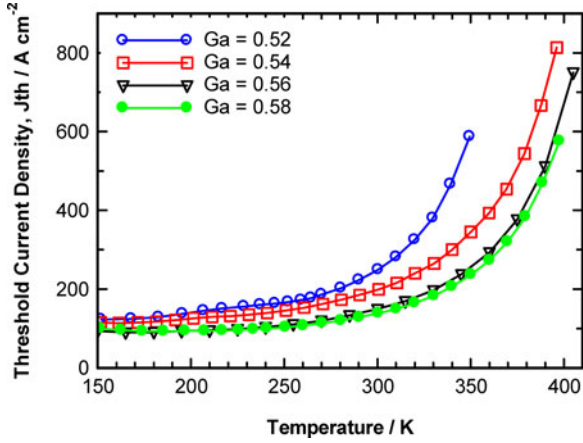


Fig. 2. Typical threshold current density versus operating temperature for 2 mm long lasers with uncoated facets with  $\text{Ga}_{a(x)}\text{In}_{(1-x)}\text{P}$  composition in the UCL of  $x = 0.52, 0.54, 0.56$  and  $0.58$ .

have as-cleaved, uncoated facets and are operated pulsed with a pulse length of 1000 ns and a duty cycle of 0.1% to avoid self-heating.

Threshold current density is measured for 2 mm long lasers and plotted in Fig. 2 as a function of heatsink temperature. The data exhibits a typical non-linear increase of threshold current density as a function of temperature for all of the Ga concentrations,  $x$ , in the UCL. Lasers with a composition of  $x = 0.58$  have the lowest threshold current density across the temperature range 240–400 K. Thresholds decreased as gallium fraction increased: at 300 K a value of  $138 \text{ A}\cdot\text{cm}^{-2}$  for gallium fraction  $x = 0.58$  was obtained with a slightly higher value of  $149 \text{ A}\cdot\text{cm}^{-2}$  for  $x = 0.56$ , increasing to  $186 \text{ A}\cdot\text{cm}^{-2}$  for  $x = 0.54$  and  $248 \text{ A}\cdot\text{cm}^{-2}$  for  $x = 0.52$ . At higher temperatures a similar trend was seen with a threshold current density of  $235 \text{ A}\cdot\text{cm}^{-2}$  for  $x = 0.58$  and almost as low a value of  $256 \text{ A}\cdot\text{cm}^{-2}$  for  $x = 0.56$  at 350 K (77 °C). These are record low values for this type of lasers.  $T_0$  values, which tend to be lower for low threshold current devices, for the four structures, across the temperature range 20 to 50 °C (293 to 343 K) are 63, 96, 107 and 99 K in order of increasing gallium concentration.

### III. ABSORPTION AND GAIN

While it is difficult to measure the allowed state distributions present in each of the samples we can determine the allowed state transitions by measuring absorption spectra. This is achieved here using the segmented contact method [11] allowing us to determine the internal optical mode loss,  $\alpha_i$ , and the modal absorption spectrum, the latter providing information on the magnitude and distribution of the allowed transitions in

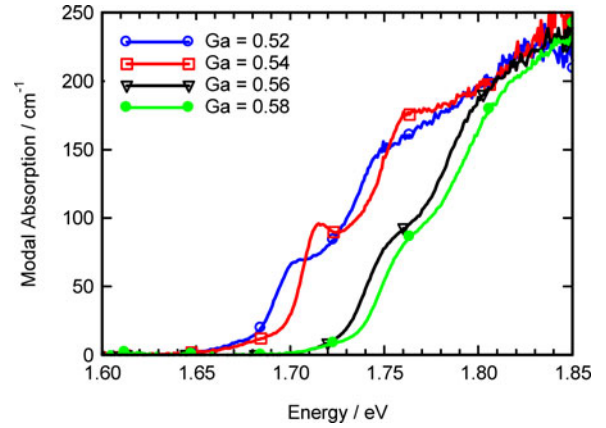


Fig. 3. Measured 300 K modal absorption spectra for samples with different Ga compositions in the UCL.

each material. In Fig. 3 we show measurements taken with the segmented contact method at 300 K for the four wafers with Ga compositions  $x = 0.52, 0.54, 0.56$  and  $0.58$ . The peaks of the ripples in the absorption spectra have previously been identified as corresponding to the inhomogeneously broadened ground state and excited state dot transitions [12]. The degree of definition of the peak indicates the degree of inhomogeneous broadening of the dot states with a better defined peak indicating a smaller dot size distribution and the magnitude of the peak (the area under the distribution is directly proportional to the number [13]) indicating the number of dots.

We note that similar spectra can be obtained as a function of temperature where a simple rigid shift in energy, according to the Varshni equation for the temperature dependence of the bandgap of the constituent materials, is the only difference between spectra. This indicates that while the bandgap decreases with increasing temperature the separation between electron states does not change significantly with temperature and a similar situation holds for hole states. We also note that the energy of the dot states at each temperature shifts according to the composition,  $x$ , and energy of the  $\text{Ga}_{a(x)}\text{In}_{1-x}\text{P}$  QW. This has previously been observed for similar samples [9] and was also confirmed here using photovoltage absorption spectroscopy data (not shown), with a constant energy separation being maintained between the well and dot states. As such we would expect an approximately equal energy spacing between the QW features or QD ground states and conclude that the sample containing nominally  $x = 0.56$  has a composition closer to that of  $x = 0.58$ .

The net modal gain spectra plotted in Fig. 4 exhibit a larger broadening than the absorption spectra due to the thermal spread of carriers over the available states and the addition of carrier density dependent homogeneous broadening. The magnitude of the peak gain is significantly smaller than the absorption from the same states due to incomplete inversion due to the thermal spreading of carriers. The spectra also exhibit a peak gain that moves to higher energy with increasing pumping due to state filling. At low energy the spectra tend towards the internal optical mode loss,  $\alpha_i$ . The value here where  $x = 0.54$  is  $2.9 \text{ cm}^{-1}$ , while values of 1.7, 0.03 and  $0.02 \text{ cm}^{-1}$  are measured for  $x = 0.52$ ,  $x = 0.56$  and  $x = 0.58$  respectively as summarised in Table I.

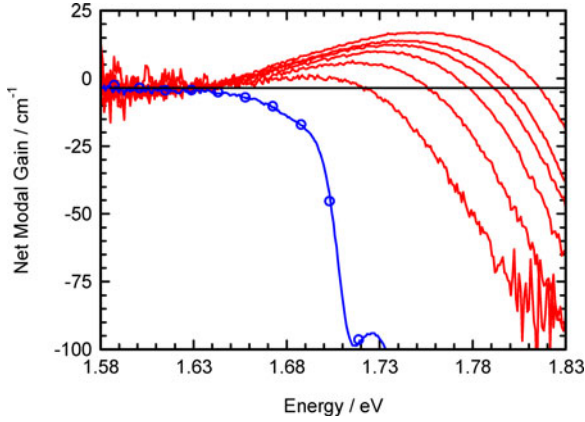


Fig. 4. Net modal gain spectra measured using the segment contact method for the Ga = 0.54 sample and for drive current densities increasing in multiples of  $111 \text{ A}\cdot\text{cm}^{-2}$  (omitting  $6\times$ ) in red and the corresponding modal absorption spectrum plotted as net modal gain in blue (with circles).

TABLE I  
MEASURED VALUES OF  $\alpha_i$  AND THE INVERSION LEVEL REQUIRED TO PRODUCE A NET MODAL GAIN OF  $6 \text{ cm}^{-1}$  AT 300 K

$x$ composition in $\text{Ga}_x\text{In}_{1-x}\text{P}$	$\alpha_i / \text{cm}^{-1}$	Inversion level required for $6 \text{ cm}^{-1}$ gain at 300K/meV
0.52	1.7	47
0.54	2.9	46
0.56	0.03	20
0.58	0.02	21

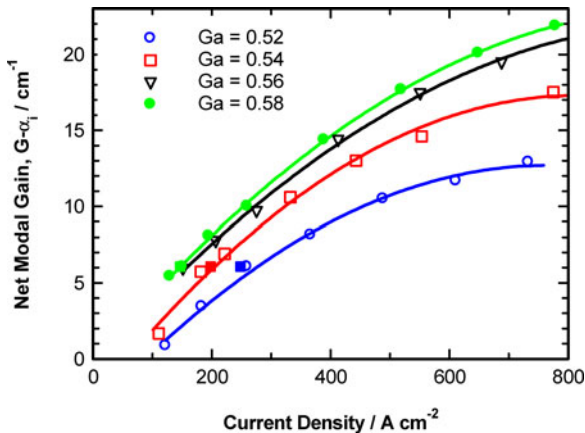


Fig. 5. Peak net modal gain taken from spectra similar to those seen in Fig. 4 for the four Ga composition samples at 300 K. (The lines are a guide to the eye).

The error in the measured value of the optical mode loss was  $\pm 1 \text{ cm}^{-1}$ . We measured no change in  $\alpha_i$  across the temperature range within error. A reduction in optical mode loss with increasing Ga fraction might be expected due to the improvement in strain balance in the structure. We have previously observed an improvement in material quality with increasing Ga fraction [9].

In Fig. 5 the peak net modal gain magnitude, taken from the data of Fig. 4 and similar data for the other samples, is plotted as a function of current density. This is the gain available to overcome the mirror loss in the laser cavity. The net modal gain is highest for the sample with  $x = 0.58$  followed by that with

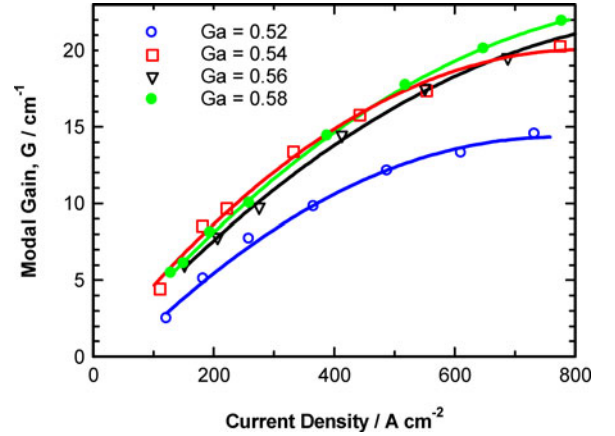


Fig. 6. Modal gain, obtained by adding the measured internal optical mode loss to the data of Fig. 5 plotted as a function of current density at 300 K. (The lines are a guide to the eye).

$x = 0.56$  with the sample with  $x = 0.52$  having the lowest peak net modal gain.

These results are consistent with the 2 mm long laser threshold current data where the gain to match the constant mirror loss of  $6 \text{ cm}^{-1}$  is required for each structure and this is achieved at the lowest current density for the  $x = 0.58$  material.

However, the value of the internal optical mode loss  $\alpha_i$ , is different for each of the samples meaning that while Fig. 5 reflects the laser results it is not necessarily reflective of the intrinsic performance of the material. The peak gain that can be achieved at a given current density is plotted in Fig. 6 by adding the experimentally determined value of  $\alpha_i$  to the data of Fig. 5. While the peak modal gain obtained from the sample with  $x = 0.52$  is still lower than that from the other samples at the same current density there is now much less difference between the other samples. In fact, at low current density the sample with  $x = 0.54$  now exhibits the largest modal gain. With no apparent trend in the values of  $\alpha_i$  of Table I, the data of Fig. 6 is probably a better representation of the intrinsic performance, or the performance that would be obtained given a large number of growths of similar designs. Having established something about the relative performance of the four samples at 300 K we now turn our attention to the temperature dependence.

#### IV. TEMPERATURE DEPENDENCE

We begin by illustrating for one temperature how the processes that lead to the temperature dependence of threshold current can be broadly characterised.

We define the inversion level (see Fig. 7: lower) as the difference between the transparency point energy ( $E_{\text{trans}}$ ) where the modal gain is zero and the absorption edge energy ( $E_{\text{abs}}$ ). The absorption edge is defined here as the energy at a fixed gain of  $-45 \text{ cm}^{-1}$ . This was selected as a fixed reference point to compare the same device at different temperatures. This is a measure of the degree of population inversion in the spirit of the text book Bernard and Duraffourg condition [14]. The data in Fig. 7 (upper figure) shows the measured modal gain and absorption spectra at the current density necessary to achieve peak net modal gain of  $6 \text{ cm}^{-1}$ , corresponding to the mirror loss

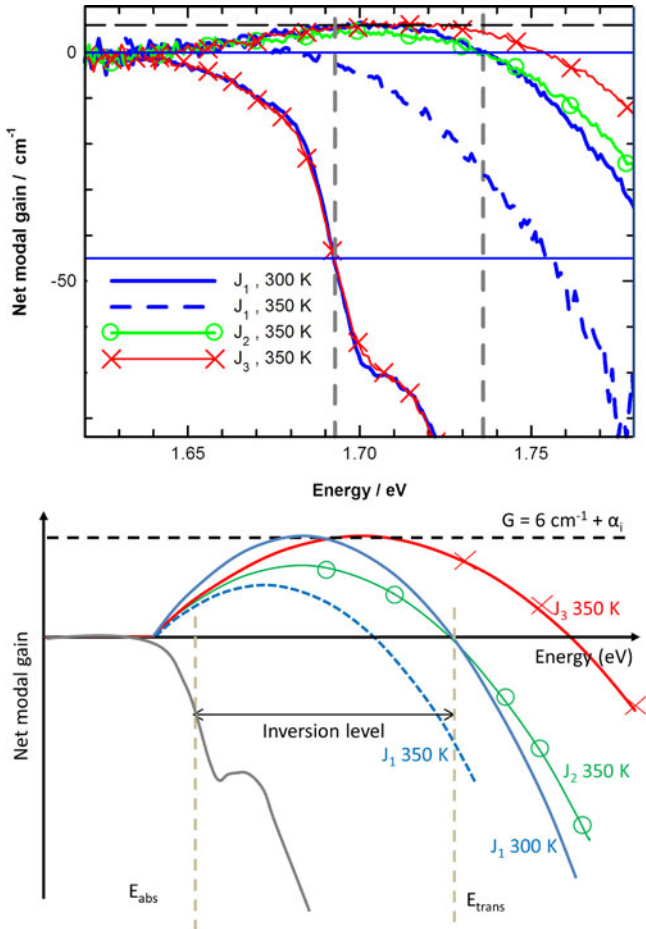


Fig. 7. Measured absorption and gain spectra at 300 K and 350 K for the sample with  $x = 0.52$  (upper). The 350 K spectra have been shifted by 23 meV so that the absorption spectra measured at the two temperatures overlap and (lower) a schematic representation of this data for clarity.

of a 2-mm-long laser, measured at 300 and 350 K. These spectra are then shown schematically in the lower figure for clarity. Two more gain spectra at 350 K are also plotted. The 350 K gain and absorption spectra have been all rigidly shifted by  $-23$  meV so that the 350 K absorption spectrum overlies the 300 K absorption spectrum, with the gain spectra shifted by the same amount. This has the effect of removing the rigid shift in both gain and absorption spectra that results from the temperature dependent shift of the bandgaps and allows spectral widths to be compared. We now separate the extra current components required at 350 K. The 300 K gain spectrum to achieve a net modal gain of  $6 \text{ cm}^{-1}$  was measured at a current density  $J_1$  (solid blue curve). The same current density  $J_1$  at 350 K produces a spectrum (dashed blue curve) with lower modal gain and reduced inversion level due to an increased carrier recombination rate. At 350 K the current density was then increased ( $J_2$ : green line with circles) to achieve the same inversion level as at 300 K, but still results in lower peak gain because the carriers are thermally spread over more energy states. Finally an increase in current density to  $J_3$  (red with crosses) achieved a peak net modal gain of  $6 \text{ cm}^{-1}$  at 350 K, with the higher inversion level necessary. We then obtain two fractions of the injected current by subtraction.  $J_2 - J_1$  is the increased pumping current to

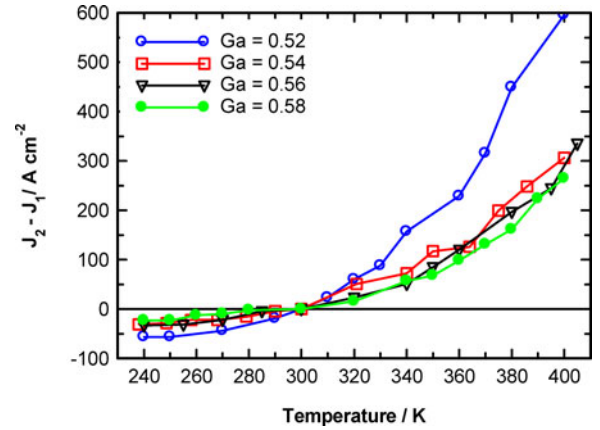


Fig. 8. The difference in current density to maintain the 300 K inversion level at each temperature and that required at 300 K ( $J_2 - J_1$ ).

compensate for the increase in radiative and non-radiative recombination from 300 to 350 K.  $J_3 - J_2$  is the extra current required for the greater energy spread of the carrier population at high temperature as described by the Fermi function. The whole process was repeated at 10 K intervals between 300 K and 400 K for all four Ga fractions. At the highest temperature measured, 400 K, for the sample with  $x = 0.52$ , 47% of the total increase in current density between 300 and 400 K ( $J_2 - J_1$ ) is required to maintain the same inversion level as at 300 K (compensate for the higher recombination rate) and 53% is required to compensate the effects of carrier spreading ( $J_3 - J_2$ ), a ratio of 47:53. For the sample with  $x = 0.58$  the equivalent ratio is 58:42. The proportion required to compensate the increased carrier spreading is now less than that required to overcome the increased recombination rate at elevated temperature. The  $x = 0.58$  current density values are dramatically lower overall than the  $x = 0.52$  values being 22% and 15% of the threshold current density for the  $x = 0.52$  sample at 400 K.

We first examine the effect of the changing recombination rate with temperature. In Fig. 8 we plot the difference between the current density required to achieve the 300 K inversion level at a given temperature and that required at 300 K ( $J_2 - J_1$ ). We see the increasing current density required at elevated temperature as already described but also that the sample with  $x = 0.52$  exhibits a current density that increases more rapidly with increasing temperature than the other samples which are all similar.

The increase in recombination with increasing temperature originates from the loss of energetic carriers from the dot states as was demonstrated using measurements of the unamplified spontaneous emission on similar samples [4]. Spontaneous emission measurements on the samples here also show appreciable spontaneous emission from, and hence population of, the well states. Such population of the QW states is a function of the inversion level (at 300 K), which is different for the different samples (see Table I). To evaluate whether the samples with different  $x$  have different recombination rates when the carrier populations are similar the current density at a single inversion level value of 46 meV (that required for the  $x = 0.52$  sample) is plotted in Fig. 9. In this case the  $x = 0.54$  sample has the lowest current density and all have similar temperature dependences suggesting that the recombination rate is lowest

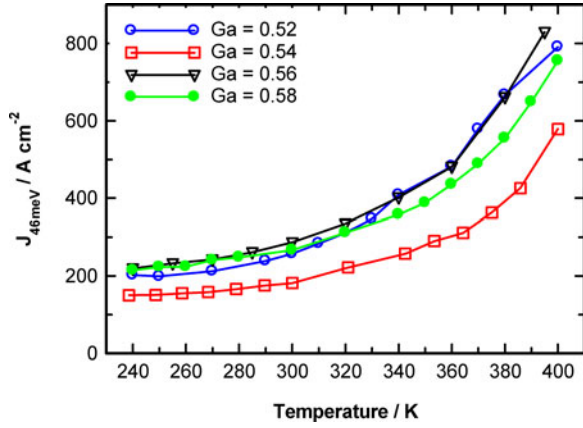


Fig. 9. The current density required to maintain an inversion level of 46 meV as a function of temperature.

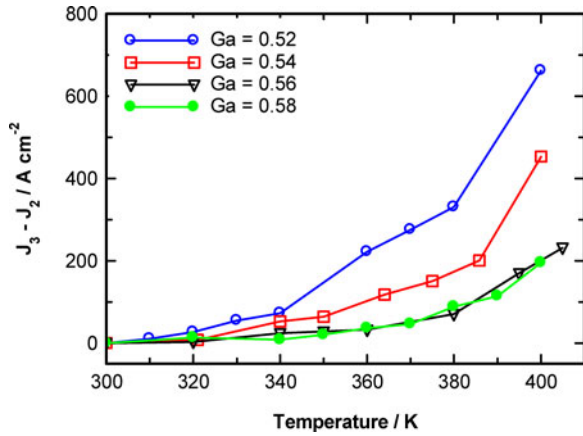


Fig. 10. Difference between the current density necessary to achieve a gain of  $6 \text{ cm}^{-1}$  ( $J_3$ ) and that to achieve the 300 K inversion ( $J_2$ ) level as a function of temperature.

in the  $x = 0.54$  material and that the temperature dependence of the recombination processes are fairly insensitive to gallium content of the UCL for the same inversion level. This must in part be due to the similar dot to well energy separation for each well composition described in Section III.

The second contribution to the current density high temperature performance arises from the current required to restore the original gain, since increased carrier spreading with temperature means the gain obtained at a given inversion level reduces. In Fig. 10 we plot as a function of temperature the difference between the current density required to achieve a net modal gain of  $6 \text{ cm}^{-1}$  ( $J_3$ ) and that required to achieve the 300 K inversion level ( $J_2$ ). The data of Fig. 10 suggests that current density increases more rapidly with temperature for the lower gallium compositions. The poorer performance of the sample with  $x = 0.52$  is thought to be due to the higher inversion level required for this sample. While the sample with  $x = 0.54$  also requires a higher inversion level this is partly mitigated by the lower recombination rate at a fixed inversion level.

To understand the role of the constituent effects we plot (see Fig. 11) the peak modal gain at the 300 K inversion level as a function of temperature for each of the samples. The samples

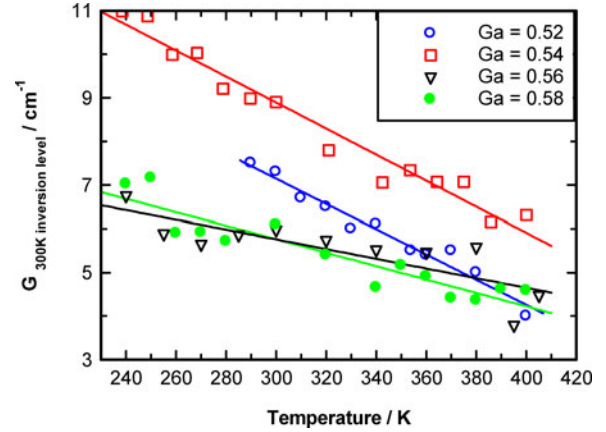


Fig. 11. Peak modal gain at the 300 K inversion level plotted (with linear fits) as a function of temperature for samples with different gallium composition in the UCL.

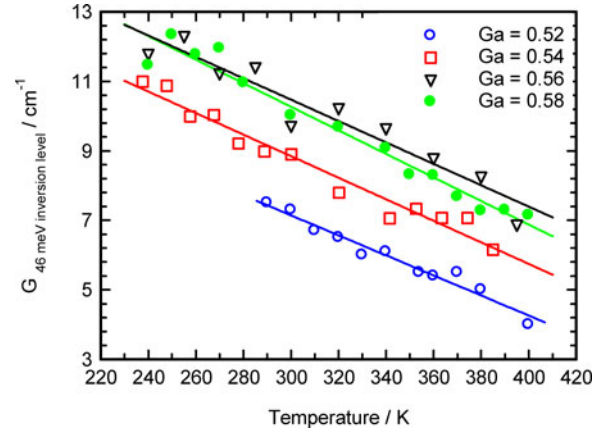


Fig. 12. Peak modal gain at the same value of inversion level of 46 meV plotted (with linear fits) as a function of temperature for samples with different gallium composition in the UCL.

with  $x = 0.56$  and  $x = 0.58$  exhibit a peak gain that changes less rapidly with temperature ( $0.011$  and  $0.015 \text{ cm}^{-1}/\text{K}$  respectively) than the samples with lower gallium compositions ( $0.029$  and  $0.030 \text{ cm}^{-1}/\text{K}$ ). However, this may in part be caused by the higher gain requirement at 300 K due to the higher values of  $\alpha_i$  and the consequential higher inversion levels for the lower gallium composition samples. To examine this we plot as a function of temperature (see Fig. 12) peak gain for a single inversion level of 46 meV. The first item of note is that gain at any temperature is increased with a higher  $x$  content, which demonstrates the value of using a higher  $x$  composition UCL, although we note that Fig. 9 also shows that the recombination current is lower for sample with  $x = 0.54$  partially negating this advantage. With respect to temperature dependence the data of Fig. 12 now shows a similar rate of decrease of gain peak with temperature for all samples ( $0.029, 0.031, 0.031, 0.034 \text{ cm}^{-1}/\text{K}$ , in order of increasing  $x$ ) and that the improved performance of the higher gallium samples seen in Fig. 11 is largely due to the lower inversion level.

While the data of Figs. 11 and 12 show the reduction in gain due to carrier spreading the temperature sensitivity of the

current is the parameter important in device operation. This can be derived by multiplying the rate of decrease of peak gain with temperature data determined above by the rate of change of current with respect to gain. At 300 K the inverse of the derivative of the gain current density curve (see Fig. 6) can be used to obtain the latter.

When the data of Fig. 11 is combined with the data of Fig. 6, at the operating point for a 2 mm laser with the  $\alpha_i$  for each sample taken from Table I, performance goes from  $1.2 \text{ A}\cdot\text{cm}^{-2} / \text{K}$  for  $x = 0.52$  to  $0.8 \text{ A}\cdot\text{cm}^{-2} / \text{K}$  for  $x = 0.54$  to  $0.3 \text{ A}\cdot\text{cm}^{-2} / \text{K}$  for  $x = 0.56$  and  $0.58$  and these numbers are in broad agreement with the data of Fig. 10. More useful, as it cannot be measured directly, is the combination of the data of Fig. 12, with the same inversion level, with the inverse of the derivative of the gain current density curve of Fig. 6. In this case the current density sensitivity to temperature for  $x = 0.54$  to  $0.58$  are very similar with  $x = 0.52$  being a factor 1.5 poorer than the rest.

Together the data of Figs. 11 and 12 suggest that the reduction in gain with increasing temperature is not a strong function of composition of the UCL beyond  $x = 0.54$  but that the greatest mitigation of the effects of reduced gain due to thermal spreading occurs by reducing  $\alpha_i$  or alternatively by operating with a low gain requirement. This reinforces the importance of  $\alpha_i$  in producing high performance QD lasers [15].

## V. CONCLUSION

Record low values of threshold current density for InP QD lasers, particularly at elevated temperature, have been presented. The best results are for samples with a composition of  $\text{Ga}_{0.58}\text{In}_{0.42}\text{P}$  in the UCL above each layer of dots. However, gain-current density data suggests that performance for samples with  $x = 0.54, 0.56$  and  $0.58$  in  $\text{Ga}_x\text{In}_{1-x}\text{P}$  would be similar were it not for the very low internal optical mode loss,  $\alpha_i$  achieved in samples with  $x = 0.56$  and  $0.58$ . Gain measured at a fixed inversion level suggests that increasing  $x$  content in  $\text{Ga}_x\text{In}_{1-x}\text{P}$  has the desired effect of boosting gain at fixed inversion level but data also shows that recombination current density is reduced for  $x = 0.54$  at 300 K and elevated temperature. Increasing recombination current density at elevated temperature due to the gain reduction caused by thermal carrier spreading is significantly reduced in samples with  $x = 0.56$  and  $x = 0.58$  but measurements at common operating points indicate that this is largely due to the reduced  $\alpha_i$  for these samples and that given the same  $\alpha_i$  samples with  $x = 0.54, 0.56$  and  $0.58$  would all benefit from reduced currents due to thermal carrier spreading compared to  $x = 0.52$ .

## ACKNOWLEDGMENT

The authors would like to thank K. Barnett for fabricating laser and test structures.

## REFERENCES

- [1] P. M. Smowton *et al.*, "InP-GaInP quantum-dot lasers emitting between 690–750 nm," *IEEE J. Sel. Topics Quantum Electron.*, vol. 11, no. 5, pp. 1035–1040, Sep./Oct. 2005.
- [2] G. Walter, N. J. Holonyak, J. H. Ryou, and R. D. Dupuis, "Coupled InP quantum dot InGaP quantum well InP-InGaP-In(AlGa)P-InAlP heterostructure diode laser operation," *Appl. Phys. Lett.*, vol. 79, pp. 1956–1958, 2001.

- [3] W.-M. Schulz, M. Eichfelder, R. Roßbach, M. Jetter, and P. Michler, "InP/AlGaInP quantum dot laser emitting at 638 nm," *J. Cryst. Growth*, vol. 315, pp. 123–126, 2011.
- [4] P. M. Smowton, S. N. Elliott, S. Shutts, M. S. Al-Ghamdi, and A. B. Krysa, "Temperature-dependent threshold current in InP quantum dot lasers," *IEEE J. Sel. Topics Quantum Electron.*, vol. 17, no. 5, pp. 1343–1348, Sep./Oct. 2011.
- [5] D. R. Matthews, H. D. Summers, P. M. Smowton, and M. Hopkinson, "Experimental investigation of the effect of wetting-layer states on the gain-current characteristic of quantum-dot lasers," *Appl. Phys. Lett.*, vol. 81, no. 26, pp. 4904–4906, 2002.
- [6] J. Ahopelto, H. Lipsanen, M. Sopanen, T. Koljonen, and H. E.-M. Niemi, "Selective growth of InGaAs on nanoscale InP islands," *Appl. Phys. Lett.*, vol. 65, pp. 1662–1664, 1994.
- [7] K. Nishi, H. Saito, S. Sugou, and J.-S. Lee, "A narrow photoluminescence linewidth of 21 meV at 1.35 μm from strain-reduced InAs quantum dots covered by  $\text{In}_{0.2}\text{Ga}_{0.8}\text{As}$  grown on GaAs substrates," *Appl. Phys. Lett.*, vol. 74, pp. 1111–1113, 1999.
- [8] L. Seravelli *et al.*, "Quantum dot strain engineering of InAs/InGaAs nanostructures," *J. Appl. Phys.*, vol. 101, p. 024313, 2007.
- [9] S. N. Elliott, P. M. Smowton, A. B. Krysa, and R. Beanland, "The effect of strained confinement layers in InP self-assembled quantum dot material," *Semicond. Sci. Technol.*, vol. 27, art. no. 094008, 2012.
- [10] G. T. Liu *et al.*, "The influence of quantum-well composition on the performance of quantum dot lasers using InAs/InGaAs dots-in-a-well (DWELL) structures," *IEEE J. Quantum Electron.*, vol. 36, no. 5, pp. 1272–1279, Nov. 2000.
- [11] P. Blood *et al.*, "Characterization of semiconductor laser gain media by the segmented contact method," *IEEE J. Sel. Topics Quantum Electron.*, vol. 9, no. 5, pp. 1275–1282, Sep./Oct. 2003.
- [12] M. S. Al-Ghamdi, P. M. Smowton, P. Blood, and A. B. Krysa, "Dot density effect by quantity of deposited material in InP/AlGaInP structures," *Photon. Technol. Lett.*, vol. 23, no. 16, pp. 1169–1171, 2011.
- [13] P. M. Smowton and P. Blood, "Quantum dot lasers: Theory and experiment," in *VLSI Micro- and Nanophotonics: Science, Technology, and Applications*, El-Hang Lee, Louay Eldada, M. Razeghi, C. Jagadish, Eds. Boca Raton, FL, USA: CRC Press, 2010.
- [14] M. G. A. Bernard and G. Duraffourg, "Laser conditions in semiconductors," *Phys. Status Solidi (b)*, vol. 1, pp. 699–703, 1961.
- [15] D. G. Deppe, K. Shavritranuruk, G. Ozgur, H. Chen, and S. Freisem, "Quantum dot laser diode with low threshold and low internal loss," *Electron. Lett.*, vol. 45, pp. 54–55, 2009.

**Makarimi Kasim** is currently working toward the Ph.D. degree at the School of Physics and Astronomy, Cardiff University, Cardiff, U.K. His research interests include the performance and physics of InP quantum dot lasers.

**Stella N. Elliott** received the B.Sc. degree from the University of Sussex, Brighton, U.K., in 1975, the M.Sc. degree from McMaster University, Hamilton, ON, Canada, in 1982, and the Ph.D. from Cardiff University, Cardiff, U.K., in 2010. Her research interests include the experimental characterization and physics of red, NIR and telecomms wavelength emitting quantum well, and quantum dot semiconductor diode lasers grown on GaAs, InP, and Si, feeding through into the design and modeling of epitaxial structures and waveguides. She is also interested in understanding the physical processes affecting the achievement of high power and the prevention of catastrophic optical facet and bulk damage.

**Andrey B. Krysa** received the Graduation degree from the Moscow Engineering Physics Institute, Moscow, Russia in 1990, and the Ph.D. degree in solid-state physics from the Lebedev Physical Institute, Russian Academy of Sciences, Moscow, in 1997. He joined the EPSRC National Centre for III-V Technologies, University of Sheffield, Sheffield, U.K., in 2001. Since then, he has been involved in the MOVPE of the group III phosphides and arsenide's.

**Peter M. Smowton** received the B.Sc. degree in physics and electronics in 1987, and the Ph.D. degree in electrical engineering from the University of Wales, Cardiff, U.K., in 1991. He is currently a Professor of optoelectronic devices at the School of Physics and Astronomy, Cardiff University. His research interests include the design, fabrication, and characterization of optoelectronic devices. His current research interests include QD lasers and integrated structures.